6ICEGE 6th International Conference on Earthquake Geotechnical Engineering
1-4 November 2015
Christchurch, New Zealand

Simple Formulation of the Ultimate Lateral Resistance of Single Pile in Cohesive Soils based on Active Pile Length

M. R. Aglipay[1], K. Konagai[2], T. Kiyota[3], H. Kyokawa[4]

ABSTRACT

Flexible piles subjected to a lateral load deform prominently near the ground surface and the pile deformation decreases with increasing depth. This significant deformation is called the active pile length, L_a. During a nonlinear event, a soil wedge is pushed up in the passive region along this active pile length. To investigate if the active pile length can describe the ultimate side soil reaction, a numerical simulation of single pile embedded in homogeneous cohesive soil is done using the 3D OpenSeesPL. The elasto-plastic behavior of the soil is modeled using the Von Mises multi surface kinematic plasticity model while the pile is modeled using elastic beam-column elements. From the results of the rigorous solution, a simplified method to define the ultimate lateral resistance of single piles in cohesive soils using the key parameter, L_a, is presented. This method provides more practical approach in the seismic design and assessment of piles.

Introduction

Piles are usually used as deep foundations for important structures, or structures supported by weak soils. These piles are most susceptible to external lateral loads like seismic motions. With the mere presence of two elements, i.e., the soil and the pile, the lateral resistance of piles is generally governed by the soil-pile interaction. The movements of grouped piles and their side soils are mutually dependent such that when the piles' heads are laterally loaded, they are deformed relative to the deformation of the surrounding soil and vice versa.

For flexible piles commonly used in engineering practice, the deformation of a vertical beam is observed to be significantly prominent in the region near the ground surface and decreases with increasing depth (Konagai 2003). This region of significant deformation is defined as the active pile length, L_a, where the piles can be described as a cantilever beam assuming fixity at the negligible deformation point. In this study, the point of negligible deformation is defined as the 3% of the maximum pile head deformation. This L_a, noting the stiffness of the pile relative to the surrounding soil, is a parameter reflective of the soil-pile interaction. A number of cases varying the pile and soil stiffness was numerically simulated to establish the relationship between the active pile length and the ratio of the pile stiffness to the soil stiffness.

During nonlinear events like large seismic excitations, a soil wedge is pushed up along L_a. This soil wedge along L_a is indicative of the ultimate lateral resistance. Thus, it can be inferred that the ultimate lateral pile resistance can be described by a simple parameter

[1]PhD Student, Institute of Industrial Science, University of Tokyo, Tokyo, Japan, aglipay@iis.u-tokyo.ac.jp
[2]Professor, Grad School of Urban Innovation, Yokohama National Univ, Yokohama, Japan, konagai@ynu.ac.jp
[3]Professor, Institute of Industrial Science, University of Tokyo, Tokyo, Japan, kiyota@iis.u-tokyo.ac.jp
[4]Kajima Corporation, Tokyo, Japan, kyokawa@kajima.com

reflective of the soil pile interaction. Many researches (Elgamal et. al. 2009, Lu et. al 2006, Wang et. al. 2014, etc.) on soil pile interactions have been done especially in the advent of high computing powers where rigorous solutions can be done for any complex soil-pile configuration. However, it is still warranted especially in the engineering practice that simple yet high caliber solutions can be made available. Therefore, a simplified expression using L_a as a key parameter to describe the ultimate lateral resistance of single pile embedded in cohesive soil is presented for more practical approach in the seismic design and assessment of piles.

Numerical Simulation

The finite element analyses were performed using a freeware called the OpenSeesPL developed by Lu et al. (2006) from University of California, San Diego. This software is specifically developed to simulate response of laterally loaded foundation system in three dimension. The following are the description of the geometrical configuration of the soil-pile configuration considered in this study.

Geometry of the Model

In view of symmetry, a half mesh is studied as shown in Figure 1. A single end bearing pile of length, L_p=30m is embedded in the soil box with a 0.03m protrusion above the ground surface to apply the lateral load. The dimensions of the soil box is 158.76m in the longitudinal side (x-axis), 79.38m in the transverse direction (y-axis) and 31m in depth (z-axis). The difference in the colors of the soil medium indicates the difference in the vertical meshing. The orange layer of the soil indicates finer meshing to have a better simulation near the ground surface. On the other hand, the blue layer indicates coarser meshing compared to the blue layer. In total, the soil-pile configuration model has 3536 (soil) and 231(pile and links) nodes and 2900 (soil) and 230 (pile and links) elements. The following boundary conditions are implemented: (1) the bottom of the domain is fixed in all axes (x, y and z axis), (2) the nodes in the side planes and the back are fixed in the x and y axes and free in the z axis and (3) to model the full mesh 3D solution, the nodes in the plane of symmetry are fixed in y-axis and free in x and z axis.

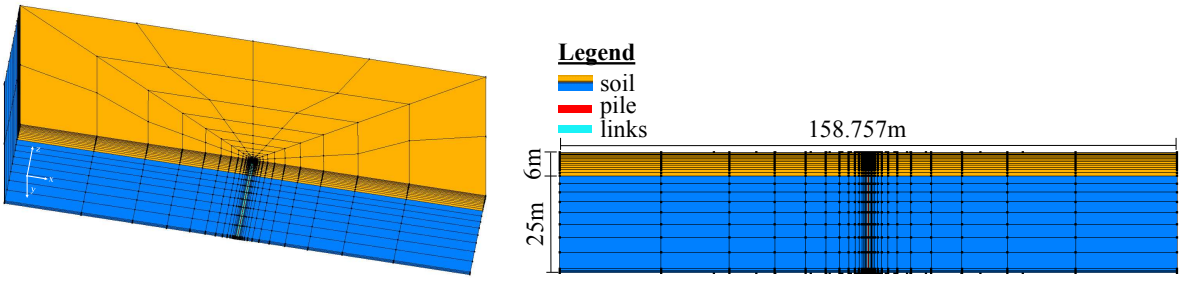

Figure 1. Soil-Pile Configuration

Soil Modeling

In OpenSeesPL, the elasto-plastic behavior of the undrained clay is captured using Prevost model (Prevost 1977). This model uses the multi-surface kinematic plasticity concept (Mroz 1967) incorporating the von Mises yield surface as seen in Figure 2.

In this case, the plasticity is observed only in the deviatoric stress-strain relationship. The

volumetric stress-strain is not affected by the deviatoric responses and exhibits a linear elastic relationship. Simply put, the constitutive model used simulates the shear behavior of clay, in monotonic or cyclic, independent of the confinement change. The backbone of the shear stress-strain curves of the clay material is modeled using the hyperbolic relationship (Kondner 1963) defined by two parameters: (1) initial tangent modulus, E_i and (2) ultimate shear strength, $(\sigma_1\text{-}\sigma_3)_{ult}$. This hyperbolic relationship is given by the following equation:

$$\sigma_1 - \sigma_3 = \frac{\varepsilon}{\frac{1}{E_i} + \frac{\varepsilon}{(\sigma_1 - \sigma_3)_{ult}}} \tag{1}$$

OpenSeesPL uses the user-defined *PressureIndependMultiYield* for clay and has a pre-defined material properties for clays as soft, medium and stiff.

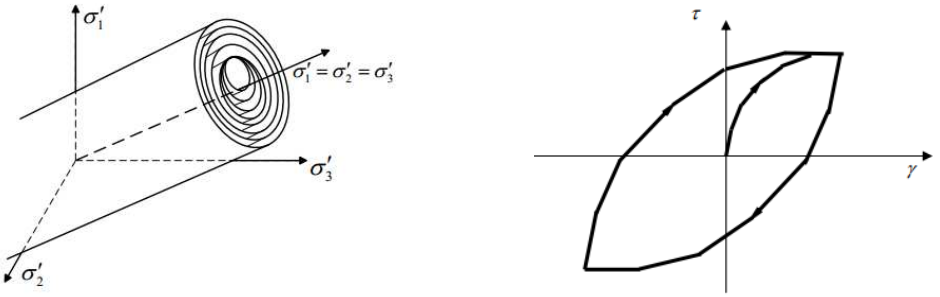

(a) Von Mises multi-surface (b) Hysteretic shear response

Figure 2. Von Mises multi surface kinematic plasticity model (after Lu et. al. 2006)

Pile Modeling

In this study, pile in elastic case is considered and uses the element type *elasticBeamColumn*. This is based on the beam-column element formulation for elastic case defined by the following parameters: (1) Young's modulus (2) poison ratio and (3) moment of inertia. Detailed information can be found in the OpenSees User Manual (Mazzoni et al. 2006).

Cases Considered

In this study, a number of static pushover tests for single end bearing pile embedded in a homogeneous clay were simulated. The static pushover test was conducted using a displacement control at pile head, where it is considered fixed. A lateral displacement is applied at the pile head at an increment of 0.001m until it reaches the final load of 1.0m. A total of 21 cases are considered in this study. The diameter of a circular pile was varied from 0.30 to 1.2m, while the Young's modulus of the pile, E_p, varied from 30GPa to 200GPa. Table 1 summarizes the different geometric and material properties of the piles used in the simulation study. These piles are embedded in soft, medium and stiff clay. The material parameters of the corresponding clay materials are given in Table 2 from the pre-defined material library of OpenSeesPL.

Table 1. Pile parameters considered

Diameter, d (m)	**Young's modulus, E_p (GPa)**	**Pile stiffness, EI_p (N-m^2)**
0.30	30	1.193 E + 07
0.50	30	9.204 E + 07
0.70	30	3.536 E + 08
1.00	30	1.473 E + 09
1.20	30	3.054 E + 09
Diameter, d (m)	**Young's modulus, E_p (GPa)**	**Pile stiffness, EI_p (N-m^2)**
0.30	200	7.952 E + 07
0.50	200	6.136 E + 08

Table 2. Soil parameters considered

Clay	**Undrained Cohesion c_u (kPa)**	**Shear modulus G_{max} (MPa)**	**Bulk modulus B (MPa)**	**Permeability coeff. (m/s)**	**Unit weight, γ (kN/m^3)**
Soft	18	13	65	1.0 E-09	11.57
Medium	37	60	300	1.0 E-09	13.55
Stiff	75	150	750	1.0 E-09	16.01

Active Pile Length

In this study, L_a is defined from the ground surface down to the point where the deformation is equal to 3% of the pile head deformation. Along this length, the pile can be described as a cantilever beam, assuming fixity for the deeper region of negligible deformation. In common engineering practice, Chang's formula (Chang 1959) given by Equation 2 is used to define the characteristic length, $L_o = 1/\beta$.

$$\beta = \sqrt[4]{\frac{k_h d}{4EI_p}} \tag{2}$$

where in Equation 2, k_h: coefficient of horizontal subgrade reaction, d: pile diameter or width and EI_p: pile stiffness. However, we note that in $k_h d$ is not an inherent property of the soil. Thus, Konagai (2003) proposed a more rational expression given in Equation 3. This expression considers the stiffness of the pile relative to the surrounding soil.

$$L_o = \sqrt[4]{\frac{EI_p}{G}} \tag{3}$$

where EI_p: pile stiffness and G: soil shear modulus. The L_a is closely investigated on by varying the parameters directly affecting it such as the pile stiffness and soil stiffness. This is assumed to exhibit a proportional relationship with L_a, ($L_a = \alpha L_o$). The progressive L_a for the single piles of various EI_p embedded in soft, medium and stiff clay are shown in Figure 3. The y-axis indicates the depth from the ground surface. In this figure, it can be observed that for the same surrounding soil, the higher the EI_p, the longer the L_a. Conversely, for the same EI_p, the ones embedded in softer clay has longer L_a than the ones embedded in stiff clay. Differences lie in the rate of change of L_a with pile head displacements depending on the EI_p

and corresponding surrounding soil medium. To provide a clear coupled action of the pile stiffness and soil stiffness on the active pile length, L_o from Equation 3 must be defined. The shear modulus is derived accounting for the shear degradation from the increase in the shear strain,γ, due to progressive pile head deformation. The derived L_o is plotted against L_a for various applied pile head displacements, particularly at 0.01m, 0.1m, 0.5m and 1.0m, as seen in Figure 4. It can be seen that there is indeed a linear relationship between L_o and L_a for various pile head displacements. Therefore from Figure 4, $L_a = \alpha L_o$ can be established.

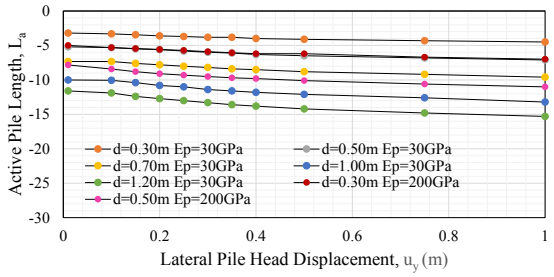

(a) Piles in soft clay

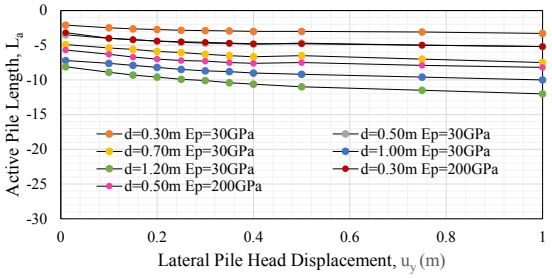

(b) Piles in medium clay

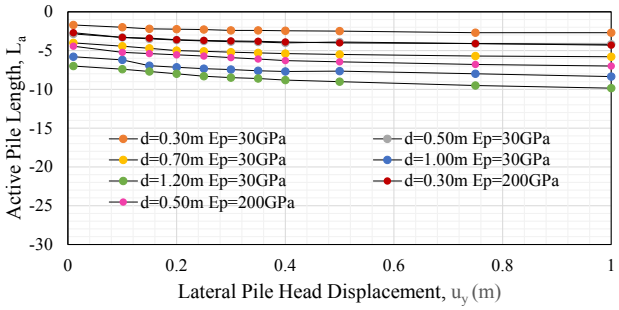

(c) Piles in stiff clay

Figure 3. Progressive active pile lengths for pile of different stiffness embedded in (a) soft clay, (b) medium clay and (c) stiff clay

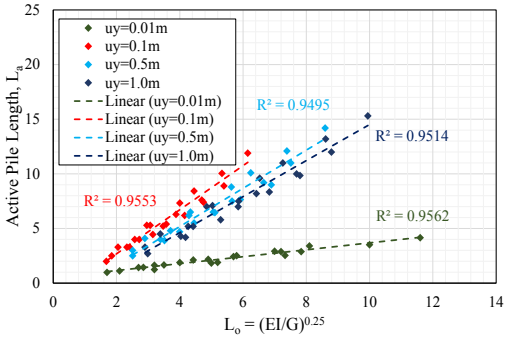

Figure 4. Relationship of L_o to L_a

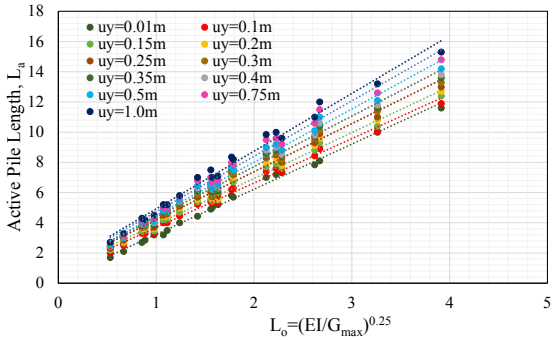

Figure 5. Relationship of initial L_o to L_a

However, it is noted that in the field, G_{max} is easily obtained. To relate this to L_a, Figure 5 is plotted. It can be seen that there is also a linear relationship with L_a and initial L_o ($L_a = \alpha L_o$), where alpha is just the slope dependent on the applied lateral pile head displacement.

Ultimate Lateral Pile Resistance

The numerical simulations show that upon application of the lateral load, a soil wedge is progressively formed at the passive region. In Figure 6, the lateral force at the pile head is given by the black line. The pile resistance based on the L_a at 0.1m (1%<γ<5%) pile head displacement is given by the blue line, where the soil wedge is deemed to be formed. The side soil reaction is derived by the difference of the lateral force at the pile head and the pile resistance. It can be observed from the side soil reaction curve, a constant line appears. This is where the ultimate lateral pile reaction is derived for all cases.

Otani (2006) investigated the failure pattern for a laterally loaded pile embedded in medium dense sand using an X-ray. His findings show that the shape of the failure wedge is a conic shape contrary to the conventional pyramidal wedge type. This study attempts to relate this conic shape to the mobilized failure wedge for laterally loaded piles embedded in cohesive soil. Since the conic wedge is mobilized along the L_a, the height of the cone is defined as L_a.

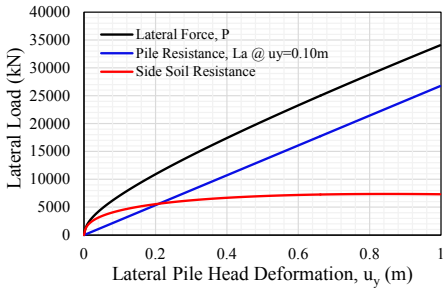

Figure 6. Load deformation curve

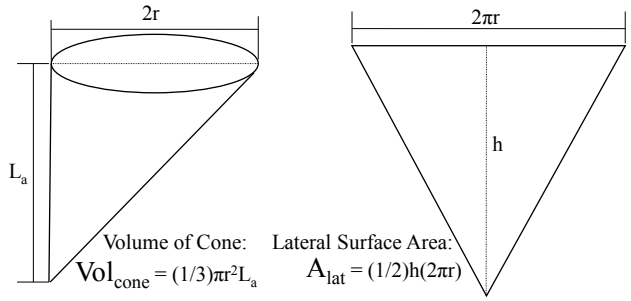

Figure 7. Conic Properties

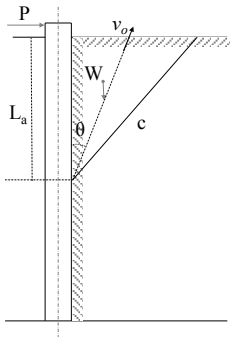

Figure 8. Soil Deformation Mechanism

Based on the energy rate equations, the governing equation is given by Equation 4. The rate of total external work done is seen at the left hand side resulting from the lateral load, P and the lifting of soil weight in the wedge, W. The right hand side of Equation 4 is the total internal energy rate dissipation at the failure surface given by C which is due to the cohesion at the failure surface.

$$P \cdot v_o \sin\theta - W \cdot v_o \cos\theta = C \cdot v_o \cos\theta \tag{4}$$

In Equation 4, v_o: the virtual velocity which can be later on cancelled and θ: half angle of the dip of the failure surface with respect to the vertical pile and dependent upon r. However, the

wedge that is discussed herein is a 3D upside-down cone, and the average θ for all directions, which is to be larger than that for 2D case, can be less dependent on r. In light of this geometric feature of the 3D cone, the dependence of equivalent $cos\theta$ and $sin\theta$ in Equation 4 for a 3D failure wedge are tentatively ignored and designated as C_0 and C_1, hereafter, for the sake of simple discussion for predominant parameter to describe ultimate side soil reaction. The weight of the soil wedge is given by the product of the unit weight of the soil and the volume of the conic soil wedge while C is given by the product of the undrained cohesion and the lateral surface area of the conic wedge. Substituting the conic properties to Equation 4, the ultimate force P from the side-soil wedge is thus given by

$$P = C_0 \cdot \gamma \cdot V_{cone} + C_1 \cdot c_u A_{lat} \tag{5}$$

where, $V_{cone} = (1/3)\pi r^2 L_a$, r: radius of the cone, c_u: undrained cohesion and γ:unit weight. A_{lat} be approximated by:

$$A_{lat} \cong \alpha \cdot 2\pi r L_a \tag{6}$$

Exactly speaking, the coefficient α depending on γ and lies within the range from 1 to $\sqrt{1+(2r/L_a)^2}$, and thus should be larger than 1. However the actual circumference of the cone's base is not completely a circle, and can be smaller than $2\pi r$. Thus for the sake of simplicity, Equation 5 is rewritten here as:

$$P = C_o \cdot \gamma \frac{1}{3}\pi r^2 L_a + C_1 \cdot c_u 2\pi r L_a \tag{7}$$

From the stress ratio distribution in the passive region as seen in Figure 9, the area of plastic formation given by the red color for piles of different diameters embedded in the same type of clay is almost the same. But the area of plastic formation for the same type of pile increases with increasing strength of clay. Thus, it is assumed that r is proportional to the soil properties: undrained cohesion and unit weight as expressed by Equation 8

$$r = \lambda \frac{c_u}{\gamma} \tag{8}$$

where λ is the proportional constant. Substituting Equation 8 in Equation 7, it is noted that

$$P \propto \frac{L_a c_u^{\,2}}{\gamma} \tag{9}$$

Based on Equation 9, the lateral force is a function of the active pile length, undrained cohesion and unit weight. Thus, these parameters are plotted against the ultimate lateral pile resistance as seen in Figure 10.

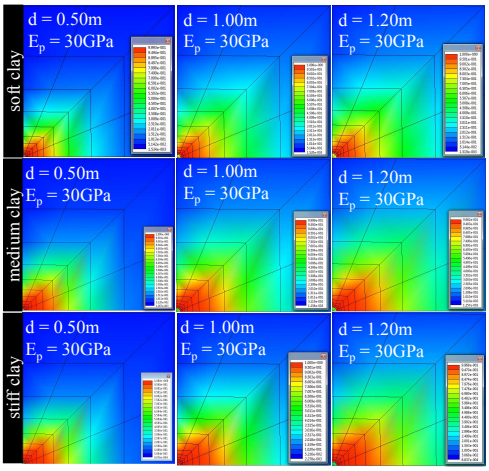

Figure 9. Stress ratio distribution for piles with diameter, d=0.5, 1.0 and 1.2m embedded in soft, medium and stiff clay in XY plane (top view)

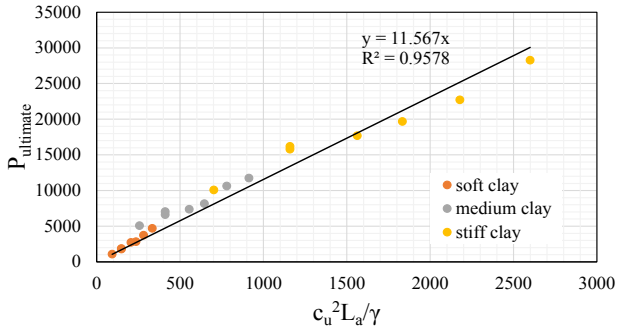

Figure 10. Relationship of $P_{ultimate}$ with L_a,c_u and γ

It can be seen that there is a high correlation between these parameters and the ultimate lateral pile resistance. There is a unique line for all the cases considered in this study varying the pile stiffness and surrounding soil. The ultimate lateral pile resistance can be empirically described by the following expression

$$P_{ultimate} = 3.68\pi \frac{c_u^2}{\gamma} L_a \quad (10)$$

Conclusions

For flexible piles, the active pile length is established to be governed by the stiffness of the pile relative to the surrounding soil stiffness. Particularly, there is a linear relationship with $(EI_p/G)^{0.25}$ for various lateral pile head displacements. This L_a can be easily defined by the initial L_o dependent on the maximum shear modulus and applying the slope of the line dependent on the applied pile head displacement. The failure wedge in the passive region can be described by a conic shape. Though a more thoughtful derivation is needed to show the predominant parameters, the numerical simulations show the potential of the idea of the use of active pile length together with other important soil parameters such as the soil unit weight and the cohesion to estimate the ultimate lateral resistance of the side soil. The verification of this idea shall be presented in the future papers. This simplified expression for the ultimate lateral pile resistance for flexible single end bearing piles can be useful for more practical

approach in the seismic and assessment of piles. This idea can be extended to a more complicated scenario i.e. non-homogeneous soil, for group piles, etc.

Acknowledgments

The author expresses thanks to the Japanese government (Monbukagakusho: MEXT) for making this study possible through their financial support.

References

Chang, YL. Discussion on lateral piles loaded tests. *Feagin Trans, ASCE*, 1937; **1959**: 272-278.

Elgamal, A, Lu J, Yang Z, Shantz T. Scenario-focused three-dimensional computational modeling in geomechanics. *Proc. 4th International Young Geotechnical Engineers' Conference*, ISSMGE, 2009.

Konagai K, Yin Y, Murono Y. Single beam analogy for describing soil-pile group interaction. *Soil Dynamics and Earthquake Engineering* 2003; **23**: 213-221.

Kondner, RL. Hyperbolic stress-strain response: cohesive soils. *Journal of Soil Mechanics and Foundations Division,* 1963; **89**: 115-143.

Lu J, Yang Z, Elgamal A. *Openseespl 3D Lateral Pile-Ground Interaction ver. 1.00 User's Manual*. Department of Structural Engineering, University of California, San Diego, La Jolla, CA, 2006.

Mazzoni S, McKenna F, Fenves GL. *Open System for Earthquake Engineering Simulation User Manual*, Pacific Earthquake Engineering Research Center, University of California, Berkeley, 2006.

Mroz, Z. On the description of anisotropic work hardening. *Journal of Mechanics and Physics of Solids* 1967; **15**: 163-175.

Otani J, Dang Pham K, Sano J. Investigation of failure patters in sand due to a laterally loaded pile using X-RAY CT. *Soils and Foundations* 2006; **46**(4):529-535.

Prevost JH. Mathematical modelling of monotonic and cyclic undrained clay behavior. *Int J Numer Anal Methods Geomech*, 1977; **1**(2):195-216.

Wang N, Elgamal A, Lu J. Three-Dimensional Finite Element Modeling of Pile and Pile Group System Response. *Soil Behavior Fundamentals to Innovations in Geotechnical Engineering* 2014; pp. 570-584.